

THE FINITE CONTACT ANGLE IN POROUS ELECTRODES AND ITS CONSEQUENCES

John O'M. Bockris and Boris D. Cahan

The Electrochemistry Laboratory
The University of Pennsylvania
Philadelphia, Pa. 19104

The theoretical solution of the porous electrode has been impeded by two major interrelated problems. The first is the choice of a proper model that is amenable to mathematical treatment, and the second is a solvable mathematical expression compatible with the physical model. The choice of a model has been tackled in several ways.

A number of authors^{1,2,etc.} have treated the entire porous electrode as a distributed network of interconnecting pores containing both fuel and electrolyte and, on some statistical basis depending on their exact choice of model, proposed any of several rate-controlling factors, and then set up equations which they then further simplified and linearized to get an analytic solution. This approach ignores the localized nature of the actual three phase region, and can lead to somewhat unrealistic models. For example, to make the mathematics easier, the random network of interconnecting passages between the particles of a sintered porous electrode is frequently 'replaced' by a set of uniform cylindrical tubes running through the porous electrode. Even forgetting that the 'real' porous structure rather resembles a three-dimensional 'string of beads', with relatively large voids interconnected by small non-circular interstices, individual pore behavior may be so dependent on pore size that it is misleading to assign some 'average' value to their diameter. 'Calibrating' factors such as 'tortuosity' can of course always be added to make the solution conform, but they rather tend to obscure the basics involved.

The other approach generally taken is to consider the local question in the meniscus region itself, and to forget the structure of the porous electrode. Thus, for example, Justi³ proposed a dissociative adsorption on the bare catalyst surface and diffusion of atomic hydrogen to the electrolyte. This treatment, however, yields far too low currents in a practical case.

Will⁴ in a paper widely quoted in recent treatments of the subject, suggested that a 'thin film' above the meniscus was the primary active region and showed good agreement with experiments using a partially immersed platinized platinum electrode. Attempts to apply this concept to 'real' electrodes leads to some inherent contradictions. In order to account for the currents produced in his meniscus, Will calculates a .5 to 1.0 μ film. But in a real porous system, where typical pore sizes are below 1 μ , this leaves no room for the gas phase, and the electrode would in effect be completely flooded. Further, since many working fuel cells are water-proofed with 'Teflon' or paraffins, a 'thin film' should be inherently unstable.

Experimental: In order to test the various theories, a simulated single pore with two-dimensional symmetry was constructed using closely spaced precision parallel plates (Fig. 1). The electrode is a sputtered Pt film (C) on an optically flat SiO₂ block (D). This block is mounted on a Teflon piston in a Teflon cell so that its spacing to an SiO₂ window (E) can be varied, thus varying the effective slit width. This geometry was chosen rather than that of capillaries because it gave a meniscus length independent of spacing, and permitted direct microscopic observation of the meniscus region.

In most cases, the Pt was in the form of a thin film sputtered onto a sub-film

of Ta, which had been sputtered into the SiO_2 electrode block. The films produced in this fashion were extremely stable and adherent, and mirror-bright. Electron microscopy showed no structure up to 150,000 X. (One of the electrodes was used for over a year, even though it was accidentally subjected to vigorous H_2 and O_2 evolution on several occasions and twice cleaned with concentrated HNO_3). Some experiments (during the initial period) were also run with a Pt foil (.005" thick) sputtered onto the face of the SiO_2 block, instead of the sputtered (2000 Å) Pt film.

The counter electrode was a thin-walled Pd tube so that any hydrogen evolved on it would diffuse into the metal, rather than be liberated as bubbles which would change the volume of the electrolyte and alter the meniscus level and/or shape. The reference electrode was a Pd-H bead to minimize contamination. This electrode retained a stability of ± 2 mv over weeks with a H_2 ambient and for better than a day with O_2 .

Runs were made both with and without special cleaning precautions. Because of the many close tolerance crevices between parts of the cell, and because of the Pd tube, the usual stringent cleaning regimes (H_2SO_4 - HNO_3 mixtures) could not be used. Instead, reagent grade isopropanol was refluxed through the assembled cell for periods up to 10 hours, and then dried for 2-3 days with a stream of highly purified N_2 . It was then washed with 1-5 liters of conductivity water distilled under N_2 directly into the cell, and the system dried again. Several additional washings were done with 5-10 cc portions of pre-electrolyzed H_2SO_4 and finally filled with fresh electrolyte, after which the cell was sealed off and the desired ambient gas introduced. After this treatment, residual currents were usually much less than 10^{-7} A/cm², and would stay so for long periods of time. A potentiostat was used to follow the voltage-current relationship using H_2 and O_2 in 1 N H_2SO_4 .

Simultaneously, measurements were made of the meniscus shape using two optical techniques. The first used interferometry with a Na "D" light to measure the thickness of the liquid in the meniscus, and in any 'thin films' which might have been present. The fringes were measured visually and by microphotography and microcinematography.

The second technique used the local curvature of the meniscus to focus the light from a point source of light into a fine line superimposed on the image of the meniscus in a microscope (Fig. 2). From the geometry, the slope of the meniscus at the locus of the line could be calculated down to and including the angle at the meniscus edge, when present. At the same time, this technique permitted an unequivocal determination as to whether a finite contact angle or a thin film continuous with the meniscus existed by the presence or absence of a critical minimum angle for the reflection at the tip.

Experimental results:

1. Optical: On the polished metal foil, and on the sputtered films which were not rigorously cleaned, the meniscus edge was always erratic and irregular and showed strong hysteresis on lowering and raising the meniscus level. After cleaning, the meniscus edge was extremely straight, any local variation from linearity usually being less than 25 μ , the limit detectable with the 60 X microscope which was used. When the meniscus was raised in the slit at a potential > 0.8 V (vs. NHE) and then lowered a 'stable' film was produced above the liquid which slowly drained to a thickness of about .5 to 1 μ . When the potential was lowered below .6 to .8 V the film split forming a finite contact angle (of between 2-6° depending on conditions), a region with a teardrop shaped cross section above it where the film had been, and a bare space between them (see Fig. 3). Once the thin film was broken, it was not possible to re-establish it except by actual re-immersion at

higher potentials. If the meniscus was lowered slowly at potentials below about .6 V, it always ran down smoothly, maintaining a finite edge, and leaving no film. (Rapid lowering of the meniscus also produced a finite edge but frequently left isolated 'islands' of solution behind.) Variation of potential in the finite edge meniscus increased the contact angle (in accordance with changes of interfacial tension changes), but it never decreased significantly unless disturbed by other causes.

2. Electrochemical: Measurements with H_2 under 'dirty' conditions were generally irreproducible and showed marked decay of current with time at constant potential. The electrode could be 'activated' by cycling it back and forth anodically and cathodically (care being taken not to evolve H_2 or O_2 on the immersed surface) but the currents from electrodes so treated dropped steadily over periods of hours.

In clean systems, erratic behavior was obtained while the 'thin films' drained, but when a finite edge was established, the currents stabilized and were generally reproducible within $\pm 2-5\%$. Occasionally, the electrodes were mildly 'activated', but the simple act of measuring the currents at potentials from 0-1 V and back sufficed for hours at a time.

Figures 4 and 5 show typical E-I curves obtained with H_2 and with O_2 at 1 atm in 1 N H_2SO_4 . Both curves show a highly linear 'pseudo-ohmic' behavior over a wide potential region. This apparent resistance (about 1000 Ω for a 1 cm long meniscus) was independent of the immersed length of the electrode. (The calculated resistance of the solution from the meniscus bottom to the bottom of the slot was only about 25 Ω in this case.) The oxygen reduction reaction was more sensitive to 'activation' than was that of hydrogen. The value of dI/dV was constant, but the intercept of I on the V axis varied with activation.

3. Meniscus heating: As reported earlier,⁵ at higher polarizations (i.e. $> \sim .5$ V) a definite activity above the meniscus was observable with the microscope. This activity took two different forms, depending on whether the system was 'clean' or 'dirty'. In the 'dirty' system, both on Pt foil and on the sputtered films, a 'fog' of minute droplets grew, coalesced and drained down into the meniscus, permitting new drops to grow in the drained regions. In 'clean' systems, a band of condensed liquid grew 25-100 μ above the meniscus edge. As the band grew, it became unstable and drained down locally into the meniscus (never draining 'dry', however) detached, and continued growing again.* This band was not continuous with the main meniscus except during the drainage, a finite edge being observable at all times.

Discussion: On the basis of the detailed physical description of the system obtained through the optical measurements, a differential equation was set up to describe the system as closely as possible. Figure 6 shows the relevant geometries involved in the 'finite contact angle meniscus'. At small pore sizes (< 1 mm), the surface of the gas-liquid interface can be represented very closely by the surface of a cylinder, the surface of which is shown as the circular arc (in cross section normal to the electrode surface). Let $x = 0$ be the point of intersection of the meniscus with the surface, the equation for the circle then becomes

$(x - x_0)^2 + (y - y_0)^2 = R^2$; at $x = 0, y = 0, R = (x_0^2 + y_0^2)^{1/2}$, and $\theta =$ contact angle $= \tan^{-1}(x_0/y_0)$. The gas (H_2) dissolves in the electrolyte and diffuses to the

⁶The phenomenon, although difficult to describe verbally, appears very similar, except in scale, to the ring of condensing alcohol observable above the meniscus in a partially filled sherry glass.

electrode. Assuming equilibrium dissolution and steady state diffusion, including a linear concentration gradient (δ is much less than .05 cm) the diffusion distance, δ , from a point 'x' at the metal lies on a radius of the circle, such that $\delta = [(x - x_0)^2 + y_0^2]^{1/2} - R$. (Note: This is not strictly true since $\nabla \cdot C \neq 0$, but quite reasonable at small x, where the 'C' is large, and unimportant at large x where 'C' is small.) At the electrode surface the gas reacts giving a local current density i_x

$$i_x = i_0 (C_x/C_0) \exp(\beta \eta_x F/RT) \quad (1)$$

(where β is a non-mechanistically significant constant, but can be varied in the solution to represent the experimental Tafel slope, and η_x is the total potential jump at the metal-solution interface).

In a thin strip 'dx' deep into liquid .1cm (into the plane of the paper) between x and x + dx (see Fig. 7) the total current $I_x + dx$ has been increased from I_x by the amount $i_x \cdot dx \cdot l$, or

$$-\frac{dI_x}{dx} = i_x \quad (2)$$

(A minus sign is used here because the ion current is produced by pos. H^+ ions, but the same equation results if the opposite sign convention is used.)

Considering the diffusion of gas to the surface (and assuming a linear case as described above)

$$i_x = \frac{DZF(C_0 - C_x)}{\delta} = -\frac{dI_x}{dx} \quad (3)$$

Considering the voltage in the solution, as the current, I_x , passes through the thin slice there will be an IR drop from x to x+dx of

$$dV_x = \frac{I_x \cdot \rho \cdot dx}{\text{area}} \quad (4)$$

Thus,

$$\frac{dV_x}{dx} = \frac{I_x \cdot \rho}{\delta_x \cdot l} \quad (5)$$

Solving eqn. (3) for C_x ,

$$\frac{C_x}{C_0} = \left(1 + \frac{\delta_x}{DZFC_0} \frac{dI_x}{dx}\right) \quad (6)$$

and putting (6) into eqn. (1)

$$-\frac{dI_x}{dx} = i_x = i_0 \left(1 + \frac{\delta_x}{DZFC_0} \frac{dI_x}{dx}\right) \exp(\beta \eta_x F/RT) \quad (7)$$

solving (7) for dI_x/dx :

$$-\frac{dI_x}{dx} = \frac{i_0 \exp(\beta \eta_x F/RT)}{1 + \frac{\delta_x}{DZFC_0} \exp(\beta \eta_x F/RT)} \quad (8)$$

Solving eqn. (5) for I_x , $I_x = -(\delta_x/\rho)(dV_x/dx)$ and differentiating,

$$-\frac{dI_x}{dx} = \frac{\delta_x d^2 V_x}{\rho dx^2} + \frac{1}{\rho} \frac{d\delta_x}{dx} \frac{dV_x}{dx} \quad (9)$$

from geometry (Fig. 5)

$$\frac{d\delta_x}{dx} = \frac{(x - x_0)}{[(x - x_0)^2 + y_0^2]^{1/2}} = \frac{(x - x_0)}{\delta_x + R} \quad (10)$$

and combining (8) and (10)

$$\frac{d^2 V_x}{dx^2} + \frac{1}{\delta_x} \frac{(x - x_0)}{(\delta_x + R)} \frac{dV_x}{dx} = \frac{\rho i_0 \exp(\beta \eta F/RT)}{\delta \left[1 + \frac{i_0 \delta_x}{DZFC_0} \exp(\beta \eta F/RT) \right]} \quad (11)$$

Matching the potential in the solution with the potential at the boundary (since the metal is considered to be equipotential),

$$\eta = V_x - E(\text{Rev. for } C_0) \quad \text{and} \quad \frac{dV_x}{dx} = \frac{d\eta}{dx} \quad (12)$$

Thus, finally,

$$\frac{d^2 \eta_x}{dx^2} = - \frac{1}{\delta_x} \frac{(x - x_0)}{(\delta_x + R)} \frac{d\eta_x}{dx} + \frac{\rho}{\delta_x} \frac{i_0 \exp(\beta \eta_x F/RT)}{\left[1 + \frac{i_0 \delta_x}{DZFC_0} \exp(\beta \eta_x F/RT) \right]} \quad (13)$$

This equation is not solvable analytically, but it was programmed in Fortran IV for solution on a digital computer. Some typical results of this computer solution are also shown plotted in Figs. 4 and 5 where the curves correspond to the experimental conditions for the experimental curves shown and show I_{total} (per cm) vs. V_{applied} . Figure 8 is a typical plot of terminal current vs. overpotential produced by the computer in this case showing the effect of variation of i_0 ($A = 10^{-3}$; $B = 10^{-6}$; $C = 10^{-9}$) holding all other 'constants' constant ($D = 1.8 \times 10^{-5}$; $x_0 = 1.7 \times 10^{-3}$ cm; $y_0 = 5 \times 10^{-2}$ cm; $\rho = 4.65 \Omega \text{ cm}$; $\beta F/RT = 60 \text{ mv}$; $Z = 2$; $C_0 = 1.2 \times 10^{-6} \text{ moles/cm}^3$).

Figures 9 and 10 are typical combined plots of the local current density (D), potential (V), the integrated current from the tip to the point 'x' (C), the local polarization power loss density, and the I^2R power loss density in the electrolyte for a particular potential ($V_{\text{applied}} = .23V$) in the case of a gas electrode in 1 N H_2SO_4 , assuming for the constants involved $D = 1.8 \times 10^{-5} \text{ cm}^2/\text{sec}$; $x_0 = 1.5 \times 10^{-3} \text{ cm}$; $y_0 = 4.3 \times 10^{-2} \text{ cm}$; $\rho = 4.65 \Omega \text{ cm}$; $\beta F/RT = 60 \text{ mv}$; $Z = 2$; $i_0 = 10^{-6} \text{ A/cm}^2$; and $C_0 = 1.2 \times 10^{-6} \text{ moles/cm}^3$ where all of the constants involved are experimentally determined. The values are plotted vs. linear distance from the tip in 9, and vs. the log of the distance in Fig. 10.

The equation has been solved for a number of variations of the experimental constants involved, but the results are too numerous to include here. Of considerable interest is the fact that the solution shows that most of the current at higher polarizations is produced within very short distances (10^{-4} to 10^{-5} cm from the tip) and that the current per cm of meniscus is relatively independent of the pore size. The obvious conclusion is that any catalyst which is any further than 10^{-5} cm from a meniscus edge is worthless at high polarizations. To test this theory, thin film electrodes have been prepared on microporous substrates which contain only 10-20 μg of Pt per cm^2 of electrode surface, but yielded currents up to 400 ma/cm^2 without showing any detectable diffusion control with H_2 , and showed 'Tafellian' behavior with O_2 up to 100 ma/cm^2 .

References

1. J. S. Newman, C. W. Tobias: JECS 109 1183, 1962.
2. K. Micka; Symposium on Fuel Cell Systems, 145th Nat. Meeting A.C.S., Sept. 8, 1963.
3. E. Justi et al., p. 33, Verlag d. Akademie d. Wissenschaften u.d. Lileratur, Wiesbaden (1959).
4. Will, F. G., JECS, 110 152 (1963).
5. Bockris, L. Nanis, B. D. Cahan, J. Electroanal. Chem., 9, 474 (1965).

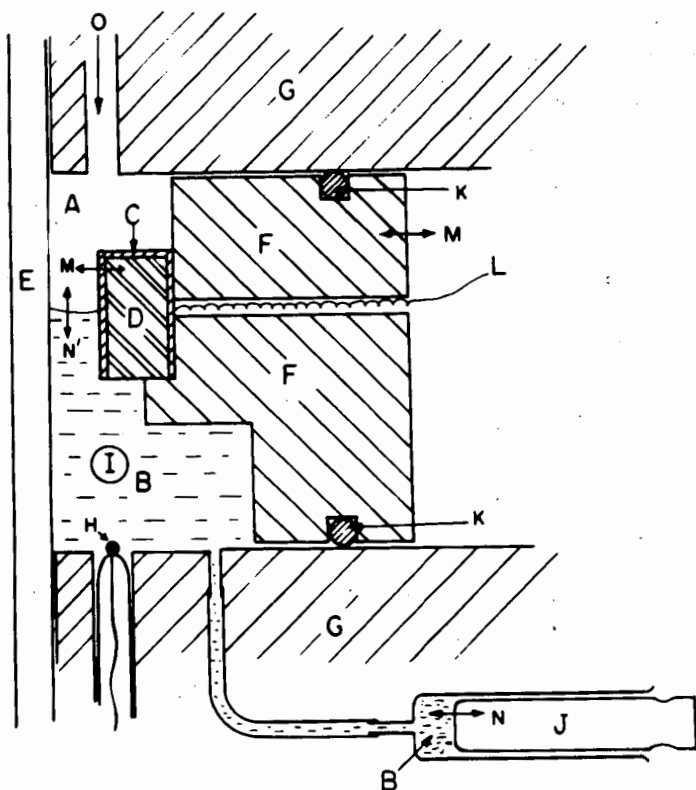


Figure 1: Cross section of slot electrode cell:

- A. Gas space
- B. Electrolyte
- C. Pt film on "D"
- D. SiO optical flat block for electrode
- E. SiO optical flat plate for window
- F. Teflon piston
- G. Teflon cell body
- H. Pd-H bead for reference electrode
- I. Pd tube for counter electrode
- J. Piston-micro-burette for changing electrolyte level
- K. O-ring seals for piston
- L. Electrical connection to rear of electrode "C"
- M, M'. In and out translation of piston varies "slot" spacing
- N, N'. Piston "J" varies meniscus level
- O. Gas inlet

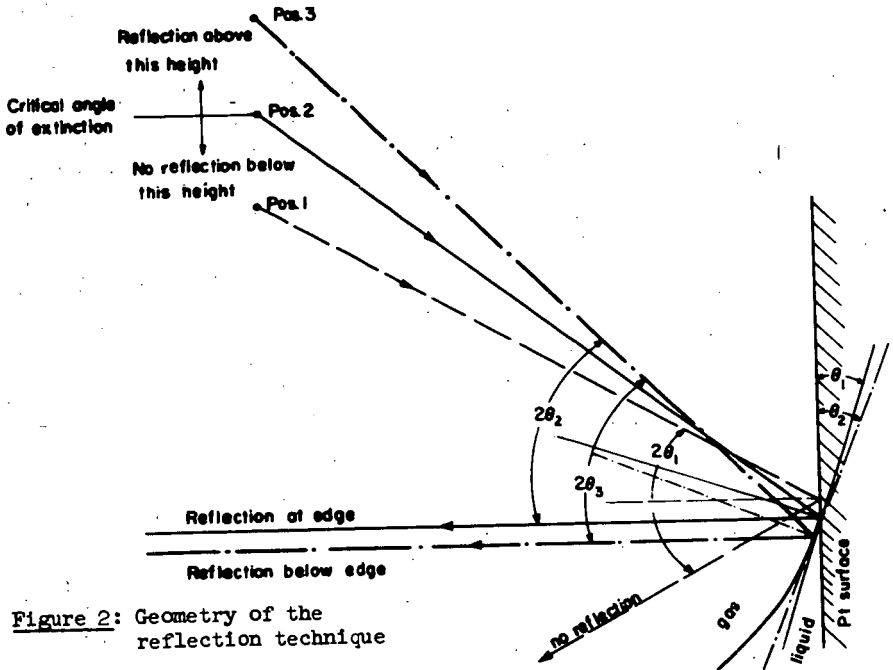


Figure 2: Geometry of the reflection technique

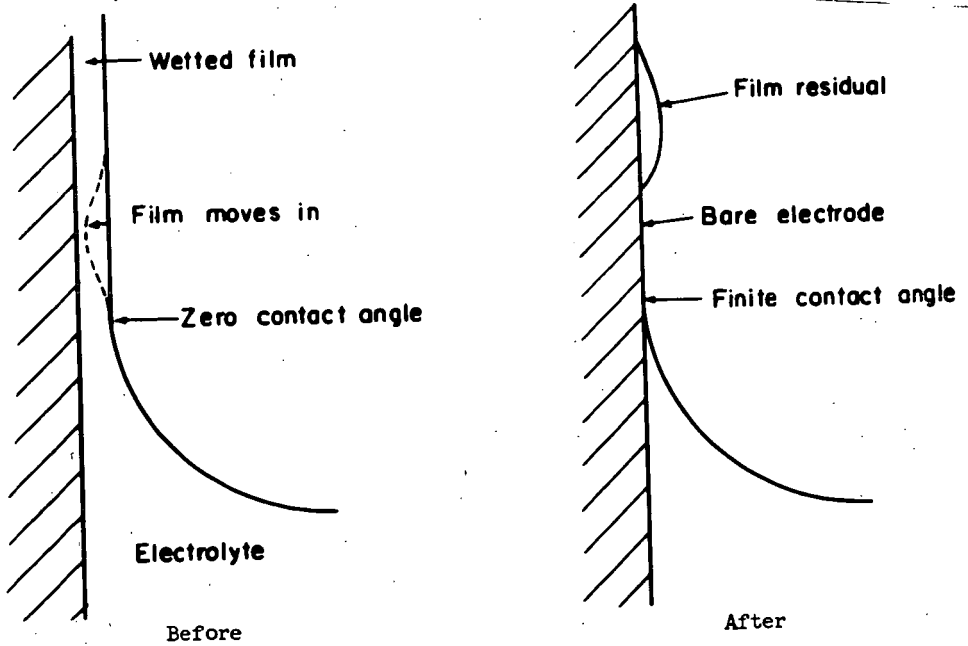


Figure 3: Creation of finite meniscus from wetted film (Horizontal dimension greatly exaggerated)

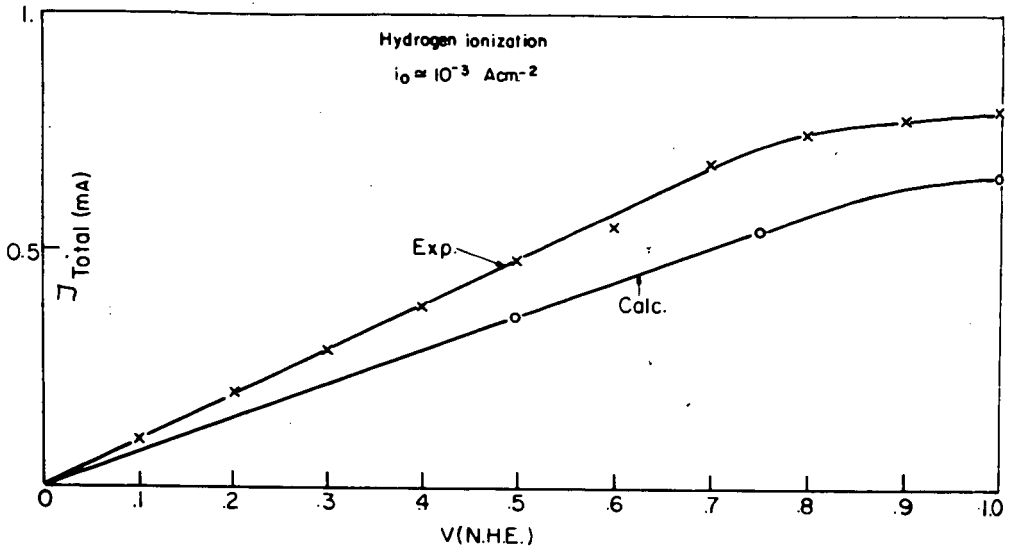


Figure 4: Experimental and calculated values for H_2

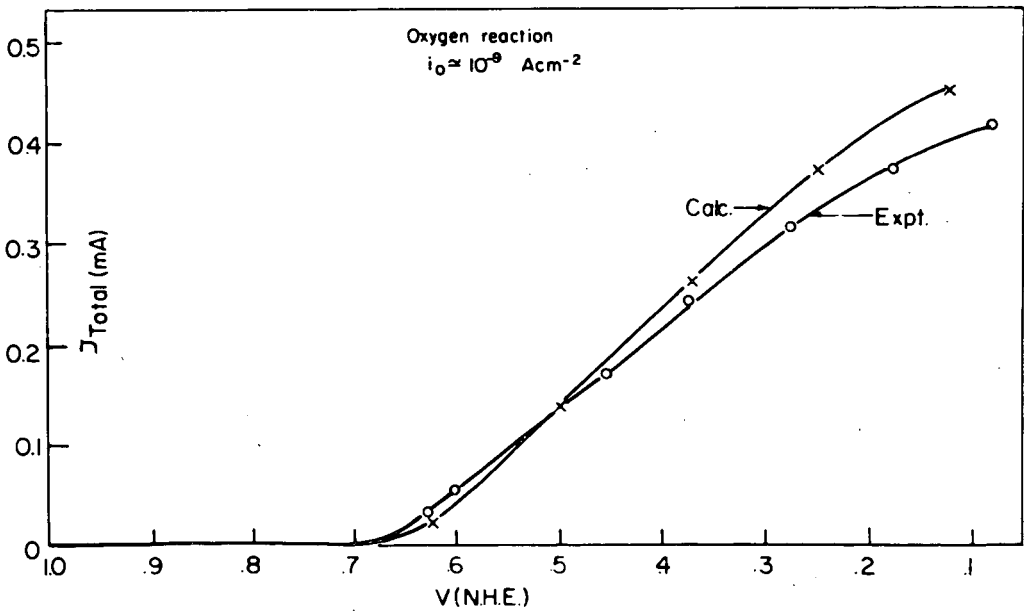


Figure 5: Experimental and calculated values for O_2

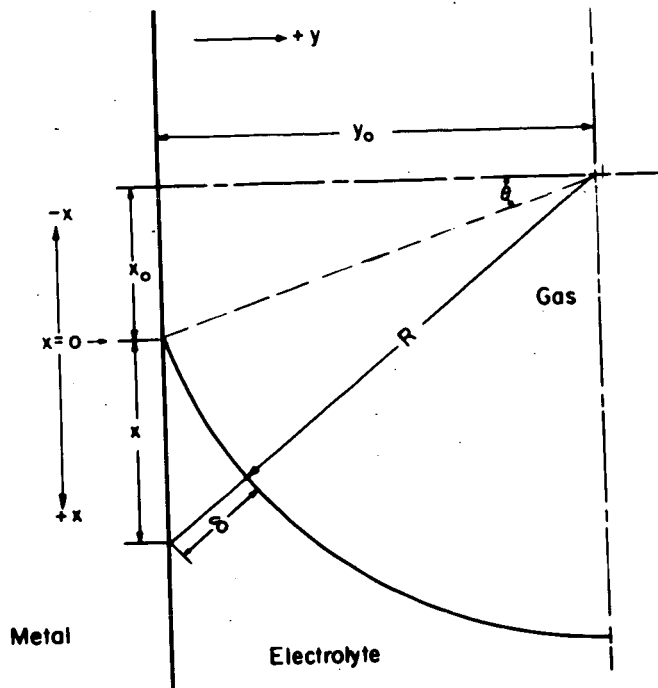


Figure 6: (above) Geometry of the meniscus for computer solution of differential equation

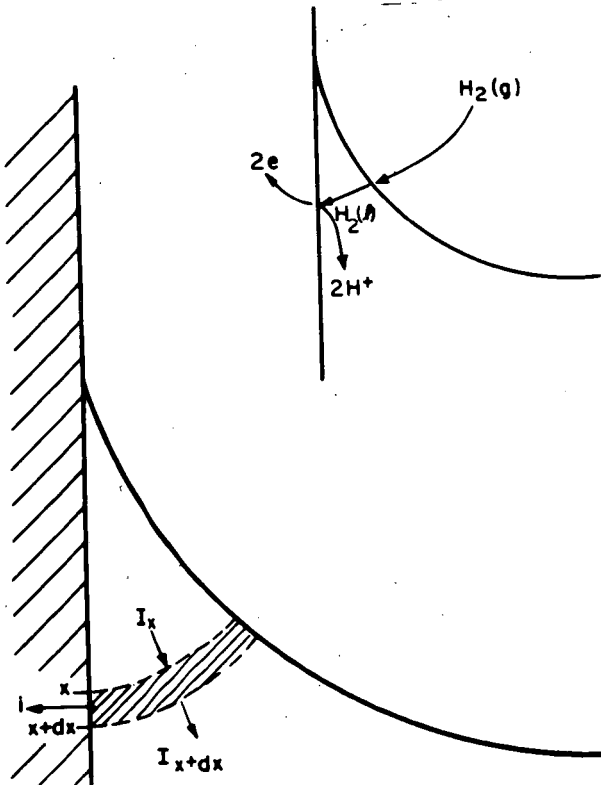


Figure 7: (left) Schematic of the flow of current and reactant

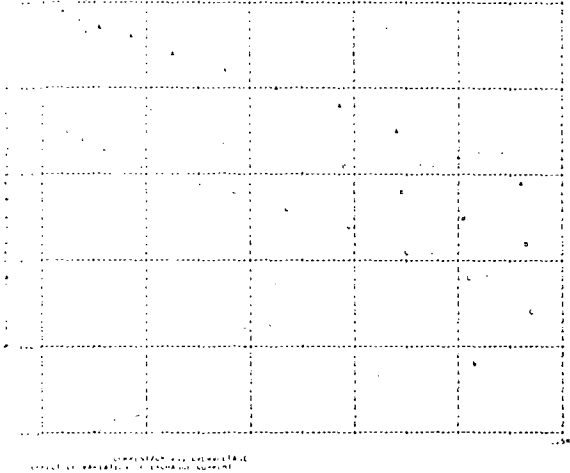


Figure 8: Computer plot of the terminal current-voltage relationship with variation of exchange current.

Curve A: $i_0 = 10^{-3}$
Curve B: $i_0 = 10^{-6}$
Curve C: $i_0 = 10^{-9}$

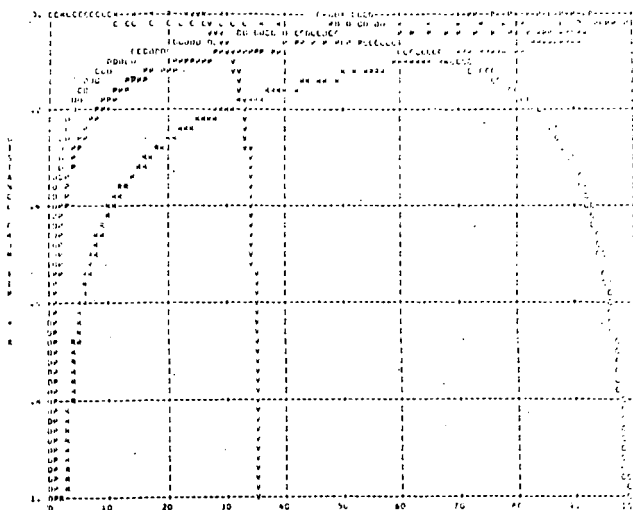


Figure 9: Computer plot of the local values of the variables in the meniscus for a given potential plotted with linear distance.

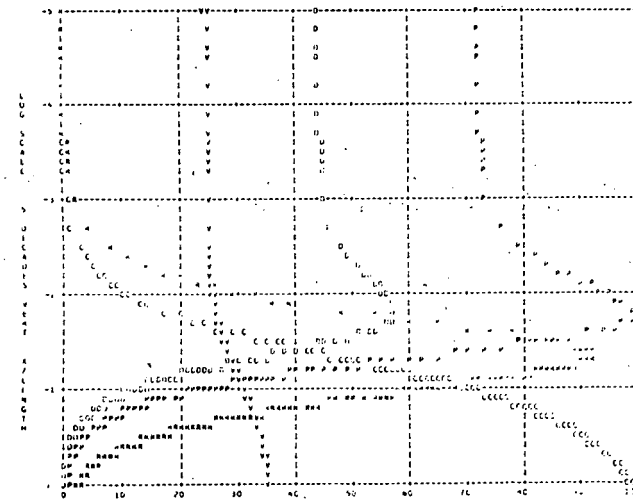


Figure 10: Computer plot of the local values of the variables in the meniscus for a given potential plotted with logarithm of the distance.